A facile synthesis of novel polyaniline/graphene nanocomposite thin films for enzyme-free electrochemical sensing of hydrogen peroxide

Swati Verma[1,2], Dipendra Singh Mal[1], Paulo Roberto de Oliveira[3], Bruno Campos Janegitz[3*], Jai Prakash[1,4*], Raju Kumar Gupta[1,5*]

[1]Department of Chemical Engineering, Indian Institute of Technology Kanpur, India-208016
[2] Department of Civil and Environmental Engineering, Hanyang University, Seoul, South Korea-04763
[3]Department of Nature Sciences, Mathematics and Education, Federal University of São Carlos, 13600-970, Araras, SP, Brazil
[4]Department of Chemistry, National Institute of Technology Hamirpur, India-177005
[5]Centre for Nanosciences, Centre for Environmental Science and Engineering, Indian Institute of Technology Kanpur, India- 208016

***Corresponding authors, *Email**: *brunocj@ufscar.br, jaip@nith.ac.in, guptark@iitk.ac.in*

Abstract

The electrochemical method is the most effective, facile, and economical approach for the detection of small molecules. The present article deals with the design and engineering of polymer-graphene-based thin films through in-situ facile synthesis technique for the development of high-performance electrochemical sensors. We report a facile technique for preparing polyaniline (PANI) and polyaniline/graphene (PANI/G) nanocomposite thin films and its application as enzyme-free electrochemical sensors for hydrogen peroxide (H_2O_2). PANI and PANI/G films were deposited on dopamine-modified ITO substrate *via* spin coating and *in-situ* deposition techniques. The *in-situ* fabricated films, which exhibited better electrical properties and stability as compared to the spin-coated films, were studied in detail. These thin films were characterized using UV-Visible spectroscopy, FT-IR spectroscopy, Raman spectroscopy, scanning electron microscopy (SEM), and atomic force microscopy (AFM) to study their optical, chemical, and surface textural properties. Results show a homogeneous distribution of constituting materials. From AFM results, it was found out that the PANI/G films showed increased surface roughness (~20 nm) as compared to the PANI film (~15 nm). The electrochemical properties of the films were determined using Van der Pauw method and cyclic voltammetry technique. The conductivity of the PANI and PANI/G films was estimated as 5.38×10^3 and 6.84×10^3 S/cm, respectively. Finally, the electrochemical sensing performances of PANI and PANI/G films were investigated towards H_2O_2 reduction in a wide potential range of -0.6 to 0.6 V in 0.1 M PBS solution of pH 7.0. This work demonstrates the application of thin-film technology for the development of nanodevice sensors.

Keywords: Thin film, polyaniline, graphene, nanocomposite, electrochemical sensing, hydrogen peroxide

1. Introduction

Hydrogen peroxide (H_2O_2) is a simple reactive molecule that plays a crucial role in chemical, biological, environmental, industrial, pharmaceutical, food, and clinical analysis [1, 2]. It is also obtained as a by-product in many enzyme-catalysed reactions like glucose oxidase, cholesterol oxidase, lactate oxidase, glutamate oxidase, etc. [3]. Because of its strong redox property, it can trigger various biological processes that can lead to different disorders in humans, such as Parkinson's, Alzheimer's, cancer, diabetes, cardiovascular and neurodegenerative disorders [4]. Therefore, monitoring H_2O_2 levels is of significant importance for both industrial and biological purposes. So far, methods that are used for the detection of H_2O_2 include fluorimetry, chromatography, spectrophotometry, chemiluminescence, and electrochemical methods [5, 6]. Among these methods, electrochemical sensing of H_2O_2 has been attracted attention from many researchers due to its high sensitivity and selectivity, rapid response, simple instrumentation, and cost-effectiveness [6, 7]. Electrochemical sensing can be performed through two types of sensors: enzymatic sensors and non-enzymatic sensors. To date, many enzyme-based sensors have been developed. They have high sensitivity and selectivity, but they have a high initial cost, complex enzyme immobilization procedure, and sometimes they present poor reproducibility and a short lifetime. This leads to the development of non-enzymatic sensors, including redox mediators, nanoparticles, carbon fillers or composites, etc.

Graphene is a promising material for various applications due to its excellent and multifunctional physical, chemical, and mechanical properties [8]. It is a conjugated network of sp^2 hybridized carbon atoms, which is accountable for its extraordinary electron transport property with the theoretical value of charge carrier mobility of the order of 2.5×10^5 cm^2 V^{-1} s^{-1}. A single sheet of pure graphene exhibits high surface area, thermal conductivity, electrical conductivity,

electron mobility, and mechanical strength [9, 10]. Graphene derivatives such as graphene oxide and reduced graphene oxide and in form of nanocomposites have also been extensively studied for various environmental remediation processes like adsorption, photocatalysis, electrochemical sensing, etc. [2, 10-14]. However, the direct use of pure graphene for such applications is restricted due to its hydrophobic character[15]. This drawback can be overcome by developing a suitable technique and methodologies that can efficiently utilize graphene or other such functional nanomaterials in its natural form without any chemical modification [16].

Polyaniline (PANI) is the polymer of aniline and is the most used conducting polymer so far because of its excellent conductive property [17]. It can exist in different forms and can have different colours depending on the extent of doping levels. Common forms of PANI polymer are leucoemeraldine, emeraldine, and pernigraniline (Scheme 1). Among these, leucoemeraldine is a non-conducting and colourless form of PANI as it is composed of fused aniline rings. Under acidic conditions, leucoemeraldine PANI can be oxidized to conducting emeraldine salt of PANI. When PANI in emeraldine base ($PANI_{EB}$) form is treated with organic or inorganic acid then emeraldine salt ($PANI_{ES}$) is formed due to protonation. $PANI_{ES}$ is a green colour compound and is the most conducting form of polyaniline. As the protonation levels in emeraldine decrease, its electrical conductivity decreases, which is also associated with a colour change phenomenon i.e., green to blue. In contrast, pernigraniline PANI and its salts are highly unstable in the presence of nucleophiles (like water) and readily decomposes in the air because of the presence of quinonediimine group.

Nowadays, the use of conductive polymers and/or conductive polymeric inks, such as PANI, has been widely used as solvent-cast for the development of 3D printing filaments. For example, the work published by Miao et al. (Miao, Z., Seo, J., & Hickner, M. A. (2018). Solvent-

cast 3D printing of polysulfone and polyaniline composites. Polymer, 152, 18-24.) that demonstrated the application of 3D filaments doped with PANI-containing inks. According to the authors, the presence of these polymers avoids printed problems attributed at high temperatures, allowing the printed process at room temperature. In addition, composite PANI-based polymer in association with metal nanoparticles has been used for preparing conductive nanofibers using the electrospinning technique. Pierini et al. (Pierini, F., Lanzi, M., Nakielski, P., & Kowalewski, T. A. (2017). Electrospun polyaniline-based composite nanofibers: Tuning the electrical conductivity by tailoring the structure of thiol-protected metal nanoparticles. Journal of Nanomaterials, 2017.) investigated the influence of electrical conductivity of nanofibers in different weight proportions of PANI and metallic nanoparticles (gold and silver) by electrospinning technique. The obtained results showed the presence of PANI in the conductive ink was able for manufacturing conductive nanofibers. Also, the polymer allowed the incorporation of metallic nanoparticles, which increased the electrical conductivity of the material.

Most of the H_2O_2 sensing studies by polyaniline/graphene (PANI/G) composites are based on the modification of glassy carbon electrodes (GCE) by the composite material. In such studies, PANI/G composite material in powder form has been deposited on the GCE with the help of gluing agents. For example, GCE modified with Ag nanoparticles decorated polyaniline/graphene composite showed promising sensing activity against H_2O_2 with a detection limit of 0.03 mM in 0.1 M PBS at pH 7.0 [11]. Similarly, Pt nanoparticles ensemble on graphene/polyaniline composites was drop-casted on GCE and used for H_2O_2 sensing in 0.1 M PBS with a detection limit of 50 nM [18]. Due to the effectiveness of the process and low detection limits, the research in the area of graphene-based electrochemical sensors is open to new strategies. In the present study, we have developed an in-situ technique for depositing thin films of PANI/G on a solid

substrate. We have used green colour PANI emeraldine salt for the fabrication of thin films because of its high electrical conductivity. The substrate material used in the present study is indium titanium oxide (ITO), which was modified using dopamine to provide adhesion between the substrate surface and films. Dopamine is a bio-inspired adhesive molecule that provides desired molecular interactions to facilitate the deposition of films on ITO substrate. The deposited films were thoroughly characterized using different spectroscopic and microscopic techniques. The films were further employed as an electrochemical sensor for the enzyme-free sensing of H_2O_2 in buffer solution. To the best of the authors knowledge, this is the first attempt to fabricate thin film-based sensors composed of PANI/G composites on ITO electrodes for H_2O_2 sensing. The novelty of this work lies in the synthesis method as these thin films were deposited on ITO under in-situ conditions to development a non-enzymatic sensor to monitor H_2O_2. To date, no such work is reported where PANI/G@ITO thin films were developed using such a technique.

2. Experimental section

2.1 Materials

Graphene nanoplatelets, aniline ($C_6H_5NH_2$, 99.5%), ammonium persulfate [$(NH_4)_2S_2O_8$], dopamine hydrochloride ($C_8H_{11}NO_2$.HCl, 98 %), hydrochloric acid (HCl, 37%), tris (hydroxymethyl) aminomethane ($C_4H_{11}NO_3$, 99.8%) were procured from Sigma Aldrich, Mumbai, India. Other chemical such as ammonia solution ($NH_3.H_2O$, 35%) was purchased from Fisher Chemical, acetone (CH_3COCH_3, 99.0%) from Emplura and ethanol (C_2H_5OH, 99%) from Ensure. All these chemicals were of analytical grade and were used directly without any purification. De-ionized water (DI water, Millipore) has been used throughout this study.

2.2 Fabrication of polyaniline/graphene films

PANI/G thin films were deposited on dopamine-modified ITO substrate by spin coating and in-situ methods. Firstly, the ITO substrate was washed with DI water followed by sonication in acetone for 10 min and dried using a nitrogen gun. For dopamine modification, ITO substrate was dipped in dopamine solution prepared by dissolving 0.1 g dopamine hydrochloride in 50 mL of 10 mM tris buffer for an hour. Then, it was rinsed with DI water and dried at 40 °C for an hour (Step 1). The role of dopamine is to provide adhesive interactions between ITO surface and PANI/G composites to enable the fabrication of stable thin films. The non-conductive side of the substrate was masked using Teflon tape before film deposition (Step 2).

In spin coating, PANI and PANI/G nanocomposites were dispersed in DMSO and spin-coated over dopamine modified ITO substrates at fixed rounds per minute (rpm) for obtaining films with uniform thickness. Detailed information on the experimental conditions used for preparing spin-coated films is given in Section 3. For the in-situ fabrication of PANI/G films on dopamine modified ITO substrate, firstly, 10 mg of graphene nanoplatelets were dispersed in 50 mL of 1.0 M HCl solution via ultra-sonication followed by the addition of 1.0 mL aniline. The obtained reaction mixture was left for ultra-sonication for an hour to obtain the uniform aniline/graphene dispersion. Ammonium persulfate (APS) solution was simultaneously prepared by dissolving 2.85 g APS in 50 mL of DI water. Both the solutions, i.e., aniline/graphene dispersion and APS solution, were kept in the ice bath for an hour before initiating the polymerization. At this stage, the dopamine-modified ITO substrate was introduced in the aniline/graphene dispersion (Step 3). APS solution was added dropwise into aniline/graphene dispersion to start the polymerization. After 10 min, ITO substrate was removed from the solution and washed with 0.2 M HCl to remove unreacted precursor materials. PANI/G coated ITO substrate was dried using a

nitrogen gun. Pure PANI film was also deposited on the modified substrate using the same procedure. PANI/G films with lower and higher graphene contents (5 & 20 mg) were also prepared similarly. Table 1 presents the thickness and conductivity data of the films prepared using various graphene contents. As can be seen, thicknesses of the films prepared using 5 and 20 mg of graphene was measured to be less than 30 nm. This could be attributed to the inappropriate graphene content, which influences the polymerization process and restricts PANI deposition on the ITO substrate. Such films were found to be unstable in solution due to lower thickness and thus were not tested for H_2O_2 sensing. In contrast, conductivity values do not seem to affect significantly with graphene content. At last, in-situ fabricated films were compared with films made by the spin coating method.

2.3. Characterization techniques

UV-visible spectroscopy was used for conducting preliminary studies of PANI/G composite using Cary 7000 Universal measurement spectrophotometer (Agilent, USA) in the wide wavelength range of 200-800 nm. Raman spectra of PANI and PANI/G composite were recorded using the Witec alpha 300 series (Witec, Germany) model with a monochromatic laser source of excitation energy of 532 nm. Various functional groups present in graphene, PANI, and PANI/G composites were analyzed by Perkin Elmer Spectrum Two FTIR spectrophotometer (Perkin Elmer, USA). For this, pellets of the samples were made with IR grade KBr and scanned in the range of 4000−400 cm^{-1}. The surface topography of the deposited PANI and PANI/G thin films was studied using JSM-7100F Scanning Electron Microscope from JEOL (JEOL, Japan) operated at 10.0 kV and using Asylum Research ARC2 Atomic Force Microscope (AFM) in tapping mode (Oxford Instruments, USA).

Optical profiling of the sample surface was performed using NanoMap–D optical profilometer to determine the thickness and roughness of thin films prepared. This technique measures the optical path difference of the sample for reference material and generates an image of the sample surface. The resistivity of the as-deposited PANI and PANI/G films on dopamine-modified ITO substrate was determined using four probes Vander Pauw method [19]. This method involves a four-point probe that was placed around the perimeter of the sample. The silver paste was applied at the corners of the thin film for making electrical contact with the probe. For making a measurement current has flowed through one edge of the sample and voltage was measured at the opposite edge. Using Ohm's law, resistance can be determined, which in turn is used to determine the conductivity of the films [20].

Cyclic voltammetry (CV) technique was used to investigate the electrochemical properties of PANI and PANI/G films along with its H_2O_2 sensing efficiency. Autolab PGSTAT302N (Metrohm, Netherlands) instrument was used to perform CV measurements using a three-electrode system. The three-electrode system comprises of as-fabricated ITO substrate as Woking electrode, Ag/AgCl/KCl as reference electrode, and Pt rod as the counter electrode. Experiments were carried out in 0.1 M phosphate buffer solution of pH 7 and in the voltage range of -0.6 V to 0.6 V at 50 mV s^{-1}. For CV and thickness measurement, an edge of the substrate was masked using Teflon tape.

2.4 Analytical procedures

The analytical performances of PANI/G and PANI modified ITO electrodes towards H_2O_2 sensing in PBS (pH=7) were examined using cyclic voltammetry. PBS of pH 7 was chosen as a working electrolyte because protonation of the emeraldine salt form of polyaniline under an acidic environment could enhance its electrical conductivity. Likewise, deprotonation of emeraldine salt

form of polyaniline in alkaline conditions could worsen its electrical conductivity. Thus, H_2O_2 sensing studies were conducted under neutral conditions to avoid any interference caused by protonation or deprotonation of polyaniline thin films. Also, sensing applications at neutral pH are scientifically more acceptable due to non-biased experimental conditions. The voltammograms were obtained by application a potential range of -0.6 V to 0.6 V at 50 mV s^{-1} in the absence and the presence of different concentrations of H_2O_2 (0 - 2.77 mM). The analytical curves were obtained by a correlation between H_2O_2 level and peak current intensity (anodic and cathodic) after signal stabilization.

3. Results and discussions

Spin-coated PANI and PANI/G films on dopamine-modified ITO were deposited at 1500 RPM for 10, 60, and 10 s as acceleration, spinning, and deceleration time, respectively. The thickness and conductivity of these films were estimated using the profilometry technique and four probes Vander Pauw method respectively (as discussed in section 3.3 in detail). The thickness and conductivity of PANI films deposited on dopamine modified ITO using the spin coater method were found to be 16 nm and 1.02E+03 S cm^{-1}, respectively. The observed decrease in conductivity as compared to in-situ fabricated films may be ascribed to the deposition of the solvent layer on the film. Similarly, PANI/G films of estimated thickness 15.2, 11, and 26.7 nm were obtained for 0.4, 0.8, and 1 mg/mL of PANI/G composites in DMSO using a spin coater, respectively. These PANI/G films also revealed poor conductivity as compared to *in-situ* fabricated films (discussed in section 3.3). Further, these films were not tested for H_2O_2 sensing due to their poor stability and peeling off the films from the ITO substrate during CV measurements. Therefore, this evidence suggests that the electrode used should be consists of the best construction configuration and composition of the proposed device. Hence, the in-situ deposited PANI and PANI/G thin films on

dopamine modified ITO substrate were mainly used for detailed characterizations and H_2O_2 sensing studies.

3.1 Chemical and molecular studies

The UV-visible spectra of in-situ deposited PANI and PANI/G thin films on dopamine modified ITO substrate is shown in **Fig. 2**. The spectrum of PANI films reveals a high-intensity absorption bands at 324 nm corresponding to π–π* electronic transitions associated with the benzenoid rings of the emeraldine salt form of PANI. It also exhibits a shoulder band at 421 nm and a rising absorption edge beyond 550 nm related to the formation of polarons and bi-polarons in the macromolecular chain of PANI, respectively. A similar pattern of peaks is also observed for PANI/G thin films with slight shifts in their positions. In the case of PANI/G thin films, the π–π* exciton peak has been observed at 317 nm with a blue shift of 7 nm. On the other hand, the absorption peak corresponding to polaron formation appears at 445 nm with a redshift of 24 nm. The observed shifts in the wavelengths could be attributed to the interaction of aromatic rings of graphene sheets with the protonated form of polyaniline. Also, the intensities of both the peaks in PANI/G thin films are low as compared to pure PANI films. The reason for this is the highly compact structure of graphene, which contributes to the low absorption efficiency of PANI/G composite and hinders the light absorption phenomenon. A rising adsorption edge corresponding to the formation of bi-polarons was also observed for PANI/G thin films beyond 490 nm. The peak corresponding to graphene (which was expected to appear around 280-285 nm) was not observed in the spectrum of the composite film due to the low concentration of graphene or due to the interference of ITO substrate at low wavelength values. Our results were similar to those reported in the literature [21, 22].

Raman spectroscopy is a powerful analytical technique for characterizing carbon-based materials. Raman spectra of PANI, graphene, and PANI/G composite are shown in Fig. 3. In the pure PANI sample, Raman peaks were observed at 1505 cm^{-1} and 1608 $cm^{-1,}$ which corresponds to C=C stretching vibrations of the benzenoid and quinoid rings, respectively. It also reveals peaks at 1345 cm^{-1} and 1169 cm^{-1} for C−C/C−N stretching vibrations and out-of-plane C−H bending vibrations modes of the quinoid rings. Other low-intensity peaks related to the out-of-plane vibrational modes associated with the deformed benzene rings were observed at 816 cm^{-1}, 522 cm^{-1}, and 407 cm^{-1}. Another low-intensity Raman band for vibrations associated with cross-linked PANI chains was observed at 586 cm^{-1} [23]. Raman spectrum of graphene nanoplatelets showed characteristic D and G bands at 1345 cm^{-1} and 1564 cm^{-1}, respectively. G-band results from the first-order scattering of the E_{2g} vibrational modes of sp^2 hybridized carbon atoms present in the graphene skeleton. However, D-band originates due to the stretching vibrations of the sp^3 hybridized carbon atoms, indicating disorders or defect present at the edges of the aromatic graphene network. The degree of disorders of the graphene system is given by the ratio of the intensities of the two peaks, i.e., by $I_D/I_{G,}$ which was determined as 0.466. Raman spectrum of graphene also exhibits a weak intensity band at about twice the frequency of D-band i.e. 2D-band at 2690 cm^{-1}, which is assigned to the second-order Raman scattering phenomenon in graphene [24]. Raman spectrum of PANI/G composites shows a series of peaks that are characteristic of PANI and graphene. The intensity of the G-band is significantly hindered in the PANI/G composite due to the possible damping of the vibrations by PANI chains. The shape of the 2D-band is broad in the case of PANI/G composite as compared to that in graphene, which reflected possible interactions between PANI and graphene nanoplatelets. Our results are consistent with those

reported in the literature [25]. Therefore, it can be concluded PANI/G thin films have been successfully deposited on dopamine-coated ITO substrate using the in-situ technique.

The FTIR spectra of pure graphene nanoplatelets, PANI, and PANI/G composites were recorded to analyse the presence of various functional groups in the samples. The FTIR spectrum of pure graphene is shown in **Fig. 4**, which did not exhibit any peak except one at 3420 $cm^{-1,}$ which could be assigned to the stretching vibration mode of the O−H group of the physically adsorbed moisture. On the other hand, the FTIR spectrum of PANI in the Emeraldine salt form reveals its characteristic pattern of peaks for various stretching and bending vibrational modes associated with its chemical structure. PANI shows peaks at 3440 cm^{-1} corresponding to the N−H stretching vibration mode. Bands at 1568 cm^{-1} and 1489 cm^{-1} were assigned for the C=C/C=N and C−C stretching vibrations modes of the quinoid and benzenoid rings. Bands corresponding to the C−N stretch of the benzenoid and quinoid rings were observed at 1294 cm^{-1}. In-plane and out-of-plane C−H/N−H bending vibrations were observed at 1131 cm^{-1} and 794 cm^{-1}, respectively [26]. The FTIR spectrum of PANI/G composites revealed a similar pattern of peaks as that of PANI and graphene. It should be noteworthy here that no apparent shifts in peak positions and changes in peak intensities were observed in the case of the composite due to low graphene content. These results are consistent with the literature [27].

3.2 Morphology, thickness, and roughness analysis

Surface morphologies of in-situ deposited PANI and PANI/G thin films were analyzed using SEM, as shown in **Fig. 5.** The SEM image of PANI thin films showed uniform deposition of polymer over the substrate. It can also be seen that the size and shape of the polymer clusters formed were uniforms throughout the film. In contrast, PANI/G films revealed deposition of polymer clusters of different shapes and sizes on the substrate. It may be due to the interaction of

graphene nanoplatelets with PANI chains resulting in the formation of clusters of uneven shapes and sizes. The presence of graphene nanoplatelets in PANI/G films is not evident from SEM images as graphene was supposed to be dispersed in the polymer matrix and might not be present on the surface [28]. Also, it can be seen that at the same magnification the surface of PANI/G films was coarse as compared to pure PANI films, which is further confirmed by increased surface roughness using AFM. AFM was also used to examine the surface morphology and to measure the surface roughness of the as-deposited thin films. AFM images of PANI and PANI/G thin films are shown in **Fig. 6** which exhibit deposition of grain-like particles to produce a thin film. These results are consistent with the SEM images as both revealed similar kinds of morphologies. The surface roughness of PANI and PANI/G films were found to be 15 and 20 nm, respectively. This slight increase in the roughness is expected to enhance the electron transport process and thus facilitating H_2O_2 sensing.

Another complementary technique that is used for the measurement of the surface roughness and thickness of the films is optical profilometry. During the in-situ deposition of the film, it was found that the thickness of the film deposited on the substrate depends upon the time spent by the substrate in the reaction mixture. The deposition of uniform films could be seen when the substrate was present in the reaction before adding the initiator, i.e., APS solution. If the substrate was introduced during the induction period i.e., 1-3 min after the polymerization starts, the thickness of the films reduces considerably. Similarly, if the substrate was introduced after 6-7 min then no films were deposited because of the absence of aniline cation radicals that are required for primary nucleation. Therefore, the introduction of the substrate before polymerization was necessary to obtain good quality and stable films. From the profilometry technique, the thickness of PANI and PANI/G nanocomposite film on ITO was estimated to be 141 nm and 126

nm, respectively with the corresponding surface roughness of 14.7 and 19.9 nm. Reduced thickness was achieved for PANI/G film, which can be correlated with the absorption of aniline monomer on the surface of graphene nanoplatelets via non-covalent interactions such as π-π interactions. Such an interaction between graphene and aniline causes a decrease in the concentration of free aniline cation radicals that are available for deposition on the substrate. Also, it is expected that the presence of graphene might be responsible for the enhanced surface roughness, which also supports the AFM results.

3.3 Determination of electrochemical properties

Vander Pauw method is used to measure the resistivity of PANI and PANI/G thin films, which in turn gives the conductivity of the films [19]. The resistivity of the as-prepared films was determined using following equation:

$$\rho = \frac{\pi d}{2ln2}(R_{AB,CD} + R_{BC,DA}).f(R_r) \quad \text{----------(1)}$$

$$R_{AB,CD} = \frac{v_{CD}}{I_{AB}},\ R_{BC,DA} = \frac{v_{DA}}{I_{BC}} \quad \text{----------(2)}$$

$$R_r = \frac{R_{AB,CD}}{R_{BC,DA}} \quad \text{----------(3)}$$

Here, ρ is the resistivity of the film in Ohm/cm, d is the thickness of the film, R is the resistance of films in Ohm, $f(R_r)$ is the Van der Pauw's function of the ratio of $R_{AB,CD}$ and $R_{BC,DA}$. The conductivity of PANI and PANI/G thin films deposited on dopamine-modified ITO substrate was found to be 5.38E+03 and 6.84E+03 S/cm, respectively. The higher conductivity for PANI/G film could be attributed to the presence of delocalised electrons in graphene structure carrying and facilitating the flow of current throughout the film. The same behavior was also observed in the paper development by [29]. The thickness of the PANI/G film was lower as compared to PANI

films, which could be another reason for high electrical conductivity. For comparison, the conductivity of PANI/G thin film prepared on unmodified or bare ITO substrate was also determined and found to be 6.82E+03 S/cm. This suggests that dopamine modification did not influence the conductivity of the film but facilitates necessary molecular interactions between film and ITO substrate. However, thin films prepared without dopamine modification were not found stable during resistivity measurements.

The electrochemical behaviour of the as-deposited thin films of PANI and PANI/G was investigated using CV. Measurements were performed in PBS at pH 7.0 and in the potential range of -0.6 V to 0.6 V at 50 mV s^{-1}. **Fig. 7** shows the cyclic voltammograms of bare ITO, dopamine modified ITO, PANI and PANI/G films on modified ITO substrates. It can be seen that bare ITO do not reveal any redox peaks in the wide potential range suggesting electro-inactivity of the substrate. For the ITO electrode modified with dopamine, a poor faradaic process was observed at +0.3 V and -0.2 V related to the oxidation and reduction process from dopamine. Similarly, poor current values for modified electrodes are attributed to the lack of conjugation in the dopamine molecule which is favourable for our application. On the other hand, a pair of well-defined distinct redox peaks can be observed for PANI film deposited on dopamine-modified ITO substrate, which signifies oxidation and reduction potentials of PANI polymer. These oxidation and reduction peaks were observed at 0.44 V and -0.32 V (*vs.* Ag|AgCl|0.1M PBS), which are in good agreement with the reported literature and the observed potential values are different from dopamine coated ITO substrate [30]. These redox peaks are attributed to the conversion of a highly conducting state of polyaniline to a semi-conducting state i.e., Emeraldine form to leucoemeraldine form. On the other hand, oxidation and reduction peaks for PANI/G film deposited on dopamine-modified ITO appeared at 0.09 V and -0.18 V (*vs.* Ag|AgCl|0.1M PBS) respectively. The observed shifts in the

redox peaks can be correlated with the interaction of graphene nanoplatelets with PANI polymer chains. It can be seen that the peak current values for PANI/G thin film are significantly higher than PANI thin films. The observed increment can be attributed to the excellent electrical conductivity of graphene which facilitates the electron transfer process at the electrode-electrolyte interface. Redox peaks for PANI/G films are observed at lower values as compared to PANI films. The observed differences between the potential values (ΔEp) were 0.35 V for oxidation peak and -0.14 V for reduction peak. The decrease of ΔEp values is clear evidence of an improved electrochemical behaviour as the presence of graphene nanoplatelets enhances the film capacity to transfer electrons [31].

3.4 Hydrogen peroxide (H_2O_2) sensing studies

The electrochemical sensing property of as-deposited films toward H_2O_2 was investigated by measuring the current responses on PANI and PANI/G films using CV. The current response on films was recorded for varying concentrations of H_2O_2 in a wide potential range of -0.6 to 0.6 V in 0.1 M PBS solution at pH 7.0. The cyclic voltammograms of PANI and PANI/G films towards H_2O_2 detection are shown in Fig. 8. In **Fig. 8 (a),** it can be seen that oxidation and reduction current peaks values of PANI thin film observed at 0.44 V and -0.32 V, respectively were decreased gradually with the addition of H_2O_2. The observed decrease in current response is attributed to the reduction in the conductivity of the peaks due to H_2O_2 sensing. As the H_2O_2 concentration was increased from 0 to 2.77 mM, the current response recorded at 0.44 V was decreased from 135.7 $\mu A/cm^2$ to 76.75 $\mu A/cm^2$. Similarly, the current response corresponding to the reduction peak observed at -0.32 V decreased from -168.94 $\mu A/cm^2$ to -91.03 $\mu A/cm^2$. Beyond 2.77 mM H_2O_2 concentration, no current response was observed due to the saturation of the electrochemical activity of the PANI films. It should be noted here that the voltage values corresponding to the

redox peak also change with increasing H_2O_2 concentration. The observed shift in the position of anodic and cathodic peaks is attributed to the reduction of H_2O_2 into OH^- ions over PANI/G thin film surface. As-generated OH^- ions increase the pH of the electrolyte solution and thus cause shifts in peaks during the H_2O_2 sensing process. Moreover, the steady shift in peak positions with increasing H_2O_2 concentration is ascribed to the increase in the amount of OH^- ions with increasing H_2O_2 concentrations. Based on this observation, a two-step mechanism has been proposed for H_2O_2 sensing by the PANI films: (i) H_2O_2 gets adsorbed on the surface of the PANI film and (ii) transfer of electrons takes place from films to H_2O_2 which resulted in the reduction of hydrogen peroxide to OH^- ions and oxidation of $PANI_{ES}$ film to the less conducting form of PANI.

On the other hand, PANI/G thin film has shown improved electrochemical properties (**Fig. 8b**) as compared to pure PANI film. In absence of H_2O_2, the anodic and cathodic current responses measured at 0.09 V and -0.18V were 324.43 $\mu A/cm^2$ and -321.78 $\mu A/cm^2$, respectively. As H_2O_2 concentration was increased from 0 to 4.25 mM, the anodic current response decreased from 324.43 $\mu A/cm^2$ to 238.86 $\mu A/cm^2$ (ΔI_{pa} = 85.57 $\mu A/cm^2$). Similarly, the cathodic current response value dropped from -321.78 $\mu A/cm^2$ to -216.12 $\mu A/cm^2$ (ΔI_{pc} = 105.66 $\mu A/cm^2$) with increasing H_2O_2 concentrations. This gradual decrease in the peak current values was attributed to the loss in the electrochemical activity of the PANI/G thin films. However, improved electrochemical activity of PANI/G thin films is attributed to the excellent electron-transport property and electrical conductivity of graphene. The sensitivity of the as-deposited thin films towards H_2O_2 sensing was determined from the linear fitting of the initial portion of the curves in the range 0.1 - 1.0 mM as shown in **Fig. 9**. The current sensitivity values observed at anode and cathode for PANI film were 18.6 and 13.1 $\mu A.L/(cm^2.mM)$, respectively. On the other hand, PANI/G film reveals a higher anodic sensitivity of 62.2 $\mu A.L/(cm^2.mM)$ and cathodic sensitivity of 36.8 $\mu A.L/(cm^2.mM)$

towards H_2O_2 sensing. It was observed that the presence of graphene significantly increases the electrical conductivity of the PANI/ITO thin films owing to the remarkable electron transport property of graphene [32]. The values of standard error in intercept (SD), the standard deviation of intercept (SD), limit of detection (LOD), and limit of quantification (LOQ) for this process were derived from the calibration plots shown in **Fig. 10** and corresponding data is presented in **Table 2**. As can be seen, LOD values for H_2O_2 sensing by PANI thin film were calculated as 0.224 mM and 0.218 mM against cathodic and anodic current responses, respectively. On the other hand, lower LOD values of 0.142 mM at the cathode and 0.104 mM at anode were obtained for PANI/G thin. This implies that the incorporation of graphene sheets not only improves the electrical conductivity of PANI/ITO thin films but also improved their sensitivity by reducing LOD. Similarly, PANI/G thin-film records lower LOQ values as compared to PANI thin films. Moreover, correlation coefficient values are higher for PANI/G thin-film indicating the suitability of these films as H_2O_2 sensors. Thus, it can be concluded that in-situ deposited PANI/G thin film exhibits enhanced electrochemical properties towards H_2O_2 sensing as compared to pure PANI film. Although these are preliminary results, the analytical performance of PANI/G/ITO sensor has shown comparable to other electrochemical sensors reported in the literature (**Table 3**), regarding some parameters, such as pH of electrolyte, technique, linear detection range (LDR), and, mainly the monitoring potential for H_2O_2 determination, which this work has presented the slightest monitoring potential.

4. Conclusions

Pure PANI and PANI/G thin films were successfully deposited on dopamine-modified ITO substrate using the *in-situ* deposition technique. Chemical analyses of the films were carried out using FTIR and Raman spectroscopy. The morphological characterization and surface

characteristics of the films were studied using SEM and AFM techniques, which revealed uniform deposition of film over the substrate. The conductivity of PANI and PANI/G thin films was determined using the Vander Pauw method and was found to be 5.38×10^3 and 6.84×10^3 S/cm, respectively. The effectiveness of as-prepared films towards non-enzymatic sensing of H_2O_2 in PBS solution using CV technique was investigated. Higher sensitivity and electrochemical response of PANI/G films were observed towards H_2O_2 sensing as compared to pure PANI film. This could be attributed to the electron transport property of graphene sheets, which acted as transport channels for the H_2O_2 molecules to reach the active sites.

Acknowledgments

The authors are thankful to IIT Kanpur India, NIT Hamirpur India, and the Federal University of São Carlos, Brazil for providing research facilities. JP thanks the Department of Science and Technology (DST), New Delhi, India for the prestigious INSPIRE Faculty award [INSPIRE/04/2015/002452 (IFA15-MS-57)] along with a research grant for this work.

Credit authorship contribution statement

Swati Verma: Experimentation and Manuscript preparation, **Dipendra S. Mal**: Data collection and Editing, **Paulo R. de Oliveira**: Reviewing and Editing, **B. C. Janegitz**: Reviewing and Editing, **Jai Prakash**: Supervision, Conceptualization, Methodology and **R. K. Gupta**: Supervision, Reviewing and Editing

Declaration of competing interest

The authors declare that they have no known competing financial interests or personal relationships that could have appeared to influence the work reported in this paper.

References

[1] Chen W, Cai S, Ren Q-Q, Wen W, Zhao Y-D. Recent advances in electrochemical sensing for hydrogen peroxide: a review. Analyst. 2012;137:49-58.

[2] Mathivanan D, Shalini Devi KS, Sathiyan G, Tyagi A, da Silva VAOP, Janegitz BC, et al. Novel polypyrrole-graphene oxide-gold nanocomposite for high performance hydrogen peroxide sensing application. Sensors and Actuators A: Physical. 2021;328:112769.

[3] Chen S, Yuan R, Chai Y, Hu F. Electrochemical sensing of hydrogen peroxide using metal nanoparticles: a review. Microchimica Acta. 2013;180:15-32.
[4] Waris G, Ahsan H. Reactive oxygen species: role in the development of cancer and various chronic conditions. J Carcinog. 2006;5:14-.
[5] Song M, Wang J, Chen B, Wang L. A Facile, Nonreactive Hydrogen Peroxide (H2O2) Detection Method Enabled by Ion Chromatography with UV Detector. Analytical Chemistry. 2017;89:11537-44.
[6] Fernandes-Junior WS, Zaccarin LF, Oliveira GG, de Oliveira PR, Kalinke C, Bonacin JA, et al. Electrochemical Sensor Based on Nanodiamonds and Manioc Starch for Detection of Tetracycline. Journal of Sensors. 2021;2021:6622612.
[7] Zhong H, Yuan R, Chai Y, Zhang Y, Wang C, Jia F. Non-enzymatic hydrogen peroxide amperometric sensor based on a glassy carbon electrode modified with an MWCNT/polyaniline composite film and platinum nanoparticles. Microchimica Acta. 2012;176:389-95.
[8] Verma S, Dutta RK. A facile method of synthesizing ammonia modified graphene oxide for efficient removal of uranyl ions from aqueous medium. RSC Advances. 2015;5:77192-203.
[9] Kumar N, Srivastava VC. Simple Synthesis of Large Graphene Oxide Sheets via Electrochemical Method Coupled with Oxidation Process. ACS Omega. 2018;3:10233-42.
[10] Lin Y-P, Ksari Y, Prakash J, Giovanelli L, Valmalette J-C, Themlin J-M. Nitrogen-doping processes of graphene by a versatile plasma-based method. Carbon. 2014;73:216-24.
[11] Li S, Xiong J, Shen J, Qin Y, Li J, Chu F, et al. A novel hydrogen peroxide sensor based on Ag nanoparticles decorated polyaniline/graphene composites. Journal of Applied Polymer Science. 2015;132.
[12] Gupta T, Samriti, Cho J, Prakash J. Hydrothermal synthesis of TiO2 nanorods: formation chemistry, growth mechanism, and tailoring of surface properties for photocatalytic activities. Materials Today Chemistry. 2021;20:100428.
[13] Singh N, Prakash J, Gupta RK. Design and engineering of high-performance photocatalytic systems based on metal oxide–graphene–noble metal nanocomposites. Molecular Systems Design & Engineering. 2017;2:422-39.
[14] Komba N, Zhang G, Wei Q, Yang X, Prakash J, Chenitz R, et al. Iron (II) phthalocyanine/N-doped graphene: A highly efficient non-precious metal catalyst for oxygen reduction. International Journal of Hydrogen Energy. 2019;44:18103-14.
[15] Yang X, Zhang G, Prakash J, Chen Z, Gauthier M, Sun S. Chemical vapour deposition of graphene: layer control, the transfer process, characterisation, and related applications. International Reviews in Physical Chemistry. 2019;38:149-99.
[16] Prakash J, Kumar V, Erasmus LJB, Duvenhage MM, Sathiyan G, Bellucci S, et al. Phosphor Polymer Nanocomposite: ZnO:Tb3+ Embedded Polystyrene Nanocomposite Thin Films for Solid-State Lighting Applications. ACS Applied Nano Materials. 2018;1:977-88.
[17] Boeva ZA, Sergeyev VG. Polyaniline: Synthesis, properties, and application. Polymer Science Series C. 2014;56:144-53.
[18] Qiu J-D, Shi L, Liang R-P, Wang G-C, Xia X-H. Controllable Deposition of a Platinum Nanoparticle Ensemble on a Polyaniline/Graphene Hybrid as a Novel Electrode Material for Electrochemical Sensing. Chemistry – A European Journal. 2012;18:7950-9.
[19] Ramadan AA, Gould RD, Ashour A. On the Van der Pauw method of resistivity measurements. Thin Solid Films. 1994;239:272-5.
[20] Matsumura T, Sato Y. A theoretical study on Van der Pauw measurement values of inhomogeneous compound semiconductor thin films. J Mod Phys. 2010;1:340-7.
[21] Goswami S, Nandy S, Calmeiro TR, Igreja R, Martins R, Fortunato E. Stress Induced Mechano-electrical Writing-Reading of Polymer Film Powered by Contact Electrification Mechanism. Scientific Reports. 2016;6:19514.

[22] Chen N, Ren Y, Kong P, Tan L, Feng H, Luo Y. In situ one-pot preparation of reduced graphene oxide/polyaniline composite for high-performance electrochemical capacitors. Applied Surface Science. 2017;392:71-9.
[23] Rajagopalan B, Hur SH, Chung JS. Surfactant-treated graphene covered polyaniline nanowires for supercapacitor electrode. Nanoscale Research Letters. 2015;10:183.
[24] Ferrari AC, Meyer JC, Scardaci V, Casiraghi C, Lazzeri M, Mauri F, et al. Raman Spectrum of Graphene and Graphene Layers. Physical Review Letters. 2006;97:187401.
[25] Wang H, Hao Q, Yang X, Lu L, Wang X. A nanostructured graphene/polyaniline hybrid material for supercapacitors. Nanoscale. 2010;2:2164-70.
[26] Correa CM, Faez R, Bizeto MA, Camilo FF. One-pot synthesis of a polyaniline–silver nanocomposite prepared in ionic liquid. RSC advances. 2012;2:3088-93.
[27] Dong Y, Zhou Y, Ding Y, Chu X, Wang C. Sensitive detection of Pb (II) at gold nanoparticle/polyaniline/graphene modified electrode using differential pulse anodic stripping voltammetry. Analytical Methods. 2014;6:9367-74.
[28] Parmar M, Balamurugan C, Lee D-W. PANI and graphene/PANI nanocomposite films—Comparative toluene gas sensing behavior. Sensors. 2013;13:16611-24.
[29] Ji Y, Qin C, Niu H, Sun L, Jin Z, Bai X. Electrochemical and electrochromic behaviors of polyaniline-graphene oxide composites on the glass substrate/Ag nano-film electrodes prepared by vertical target pulsed laser deposition. Dyes and pigments. 2015;117:72-82.
[30] Yan C, Kanaththage YW, Short R, Gibson CT, Zou L. Graphene/Polyaniline nanocomposite as electrode material for membrane capacitive deionization. Desalination. 2014;344:274-9.
[31] Bard AJ, Faulkner LR. Fundamentals and applications: electrochemical methods. 2001.
[32] Hu F, Li W, Zhang J, Meng W. Effect of graphene oxide as a dopant on the electrochemical performance of graphene oxide/polyaniline composite. Journal of Materials Science & Technology. 2014;30:321-7.
[33] Benvidi A, Nafar MT, Jahanbani S, Tezerjani MD, Rezaeinasab M, Dalirnasab S. Developing an electrochemical sensor based on a carbon paste electrode modified with nano-composite of reduced graphene oxide and CuFe2O4 nanoparticles for determination of hydrogen peroxide. Materials Science and Engineering: C. 2017;75:1435-47.
[34] Devendiran M, Krishna Kumar K, Sriman Narayanan S. Fabrication of a novel Ferrocene/Thionin bimediator modified electrode for the electrochemical determination of dopamine and hydrogen peroxide. Journal of Electroanalytical Chemistry. 2017;802:78-88.
[35] Muralikrishna S, Cheunkar S, Lertanantawong B, Ramakrishnappa T, Nagaraju D, Surareungchai W, et al. Graphene oxide-Cu (II) composite electrode for non-enzymatic determination of hydrogen peroxide. Journal of Electroanalytical Chemistry. 2016;776:59-65.
[36] Dutta AK, Das S, Samanta PK, Roy S, Adhikary B, Biswas P. Non–enzymatic amperometric sensing of hydrogen peroxide at a CuS modified electrode for the determination of urine H2O2. Electrochimica Acta. 2014;144:282-7.
[37] Guan J-F, Huang Z-N, Zou J, Jiang X-Y, Peng D-M, Yu J-G. A sensitive non-enzymatic electrochemical sensor based on acicular manganese dioxide modified graphene nanosheets composite for hydrogen peroxide detection. Ecotoxicology and Environmental Safety. 2020;190:110123.
[38] Bradshaw MP, Prenzler PD, Scollary GR. Square-Wave Voltammetric Determination of Hydrogen Peroxide Generated from the Oxidation of Ascorbic Acid in a Model Wine Base. Electroanalysis: An International Journal Devoted to Fundamental and Practical Aspects of Electroanalysis. 2002;14:546-50.

Schemes, figures, and tables

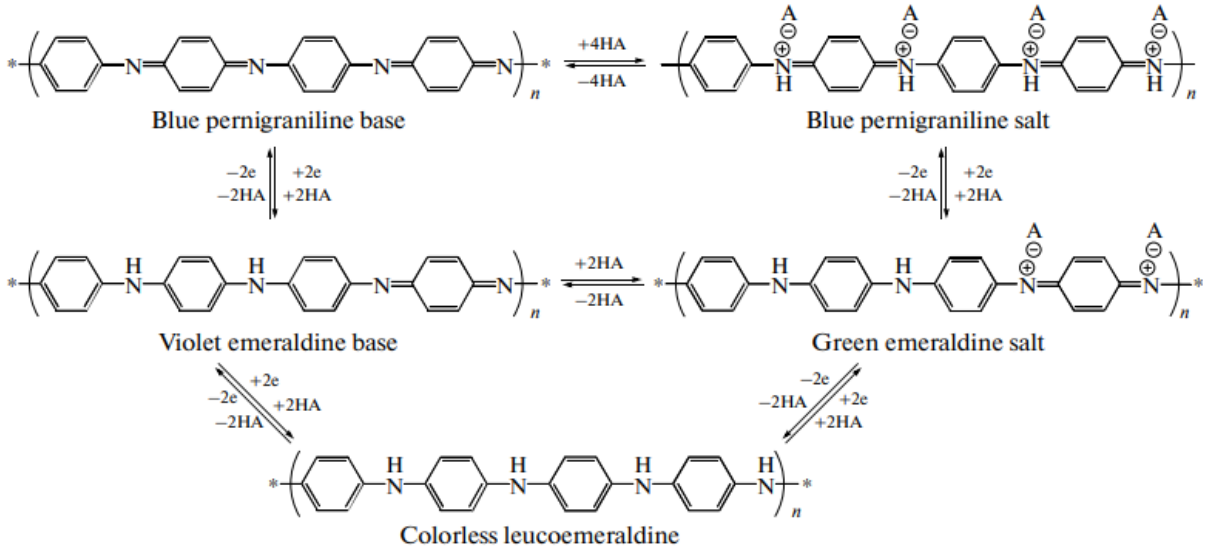

Scheme 1. Different forms of PANI polymer [17].

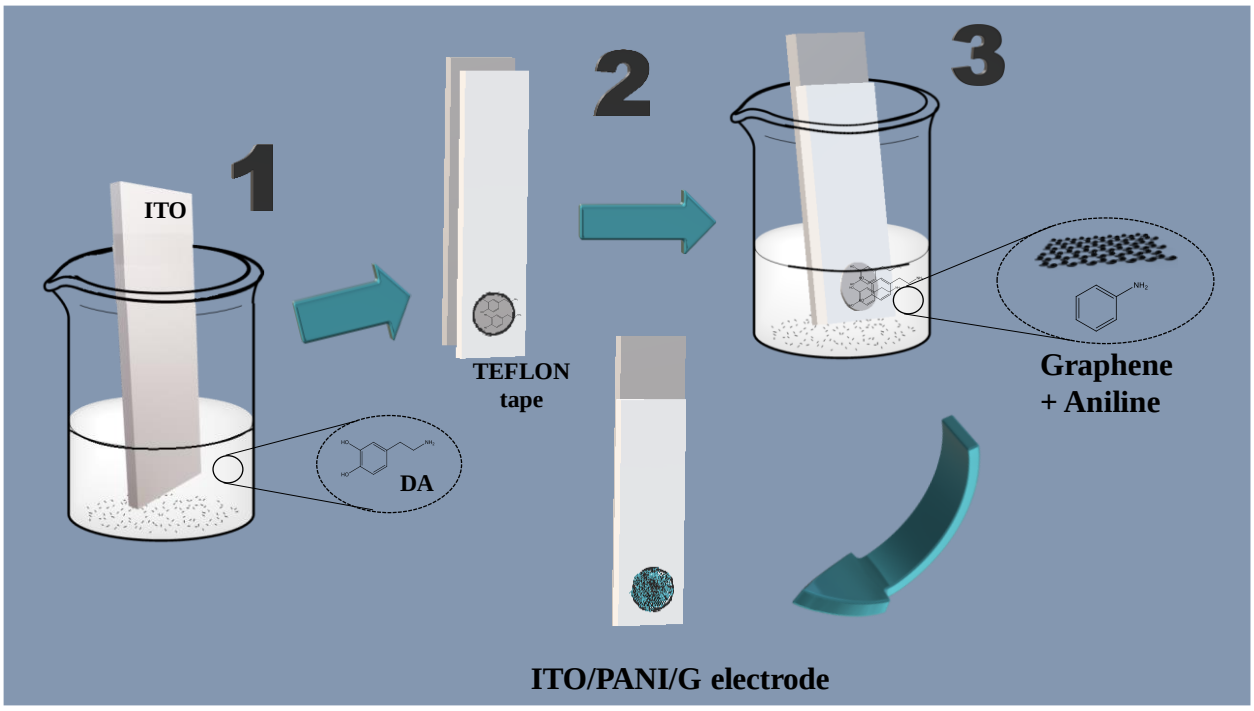

Fig. 1 Schematic step-by-step preparation of in-situ PANI/G modified electrode (PANI/G/ITO).

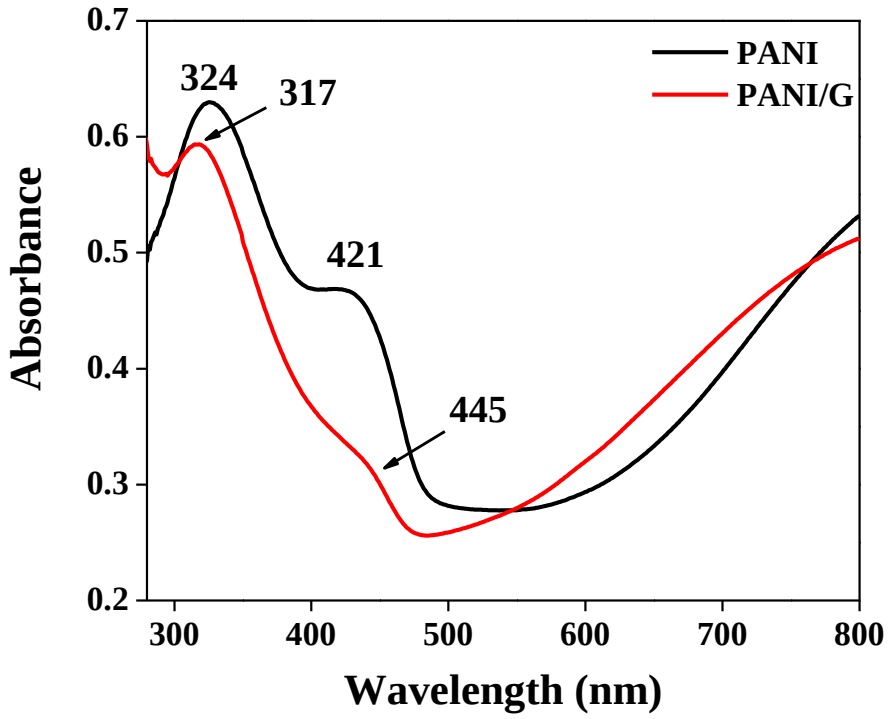

Fig. 2 UV-Visible spectra of in-situ deposited PANI and PANI/G films on dopamine modified ITO**.**

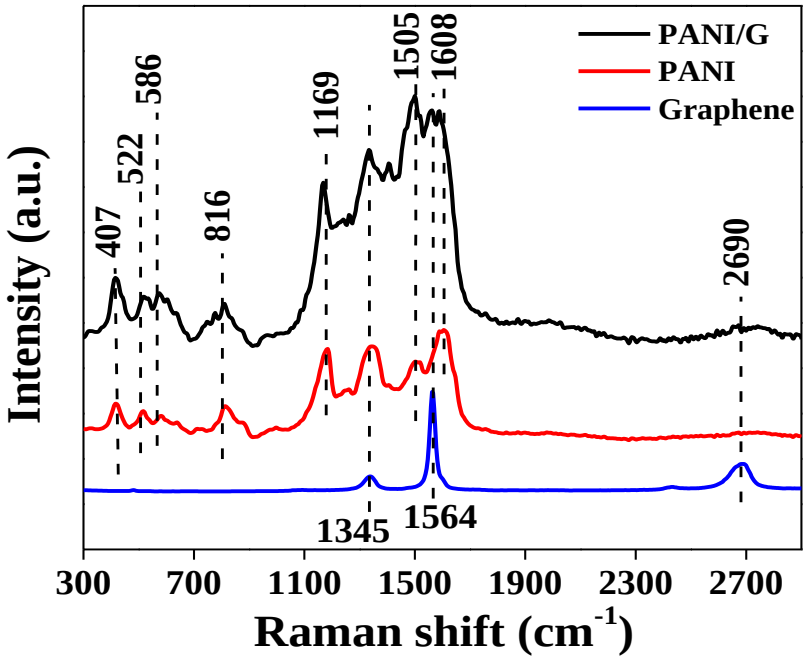

Fig. 3 Raman spectra of graphene nanoplatelets, in-situ PANI films, and in-situ PANI/G films on dopamine modified ITO.

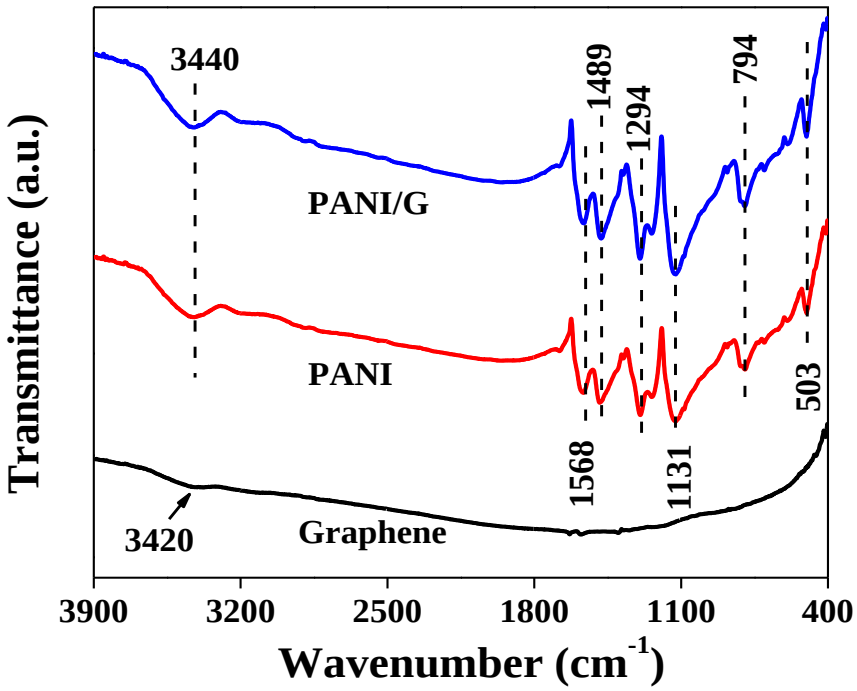

Fig. 4 FTIR spectra of graphene nanoplatelets, PANI and PANI/G composite.

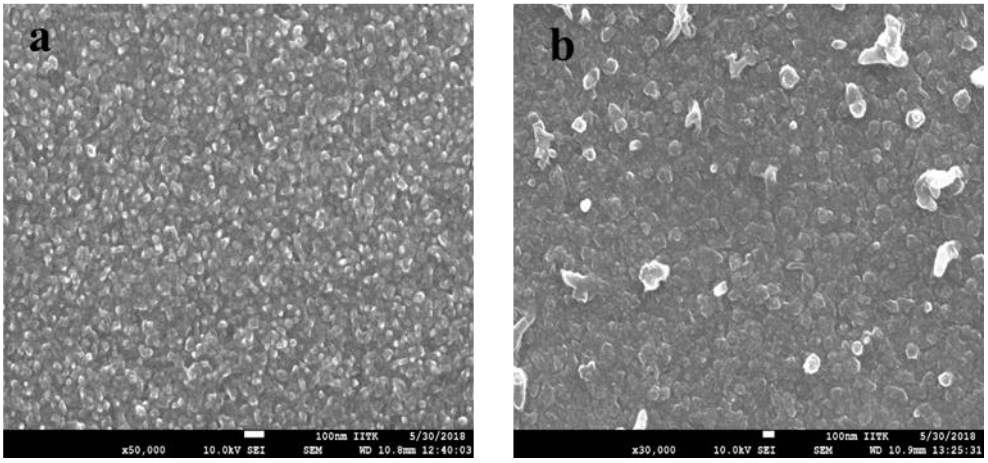

Fig. 5 SEM images of (a) PANI and (b) PANI/G thin film on dopamine modified ITO.

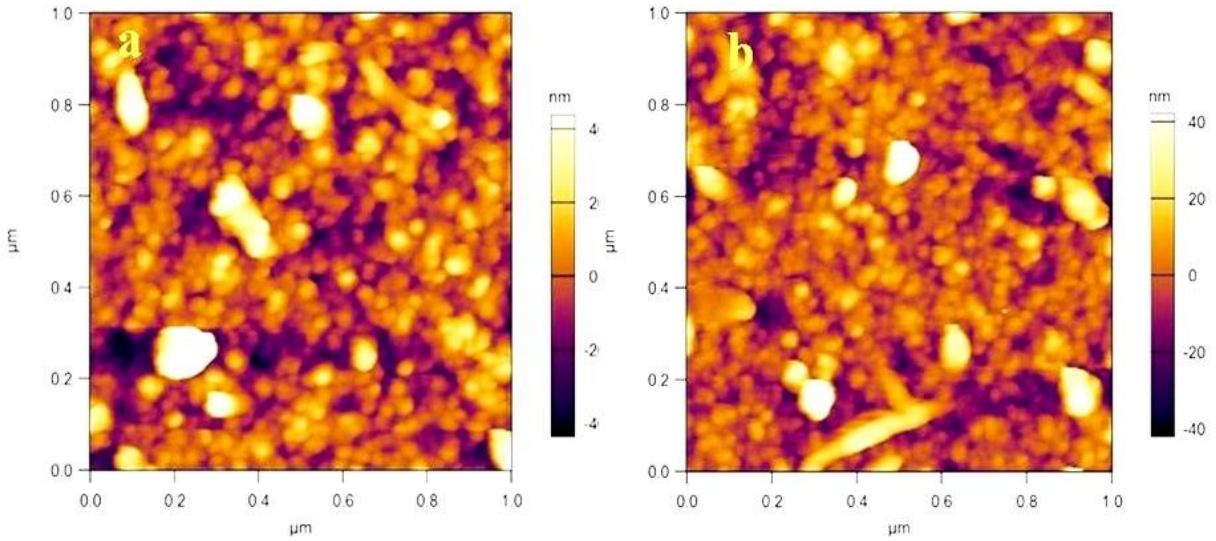

Fig. 6 AFM images of (a) PANI and (b) PANI/G thin film on dopamine modified ITO.

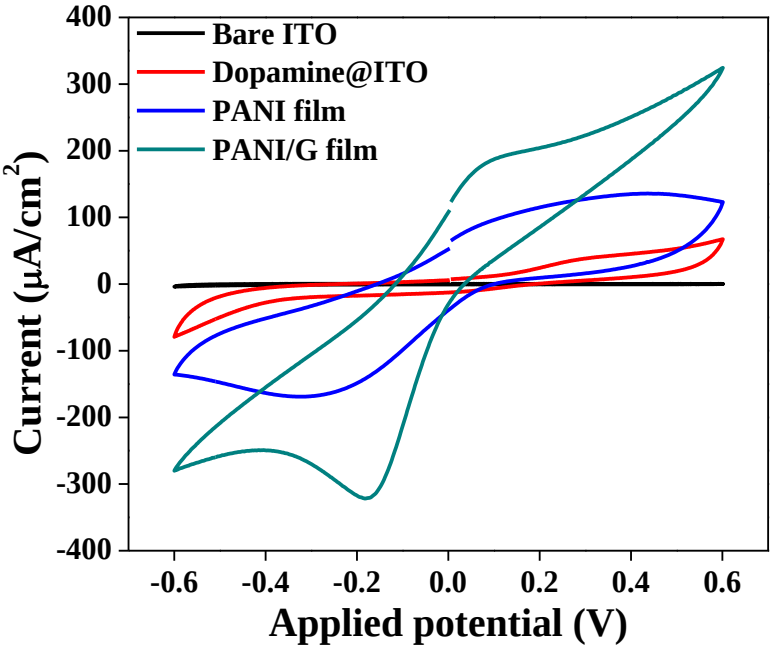

Fig. 7 Cyclic voltammograms of bare and dopamine coated ITO substrates, PANI and PANI/G thin films on dopamine coated ITO substrates.

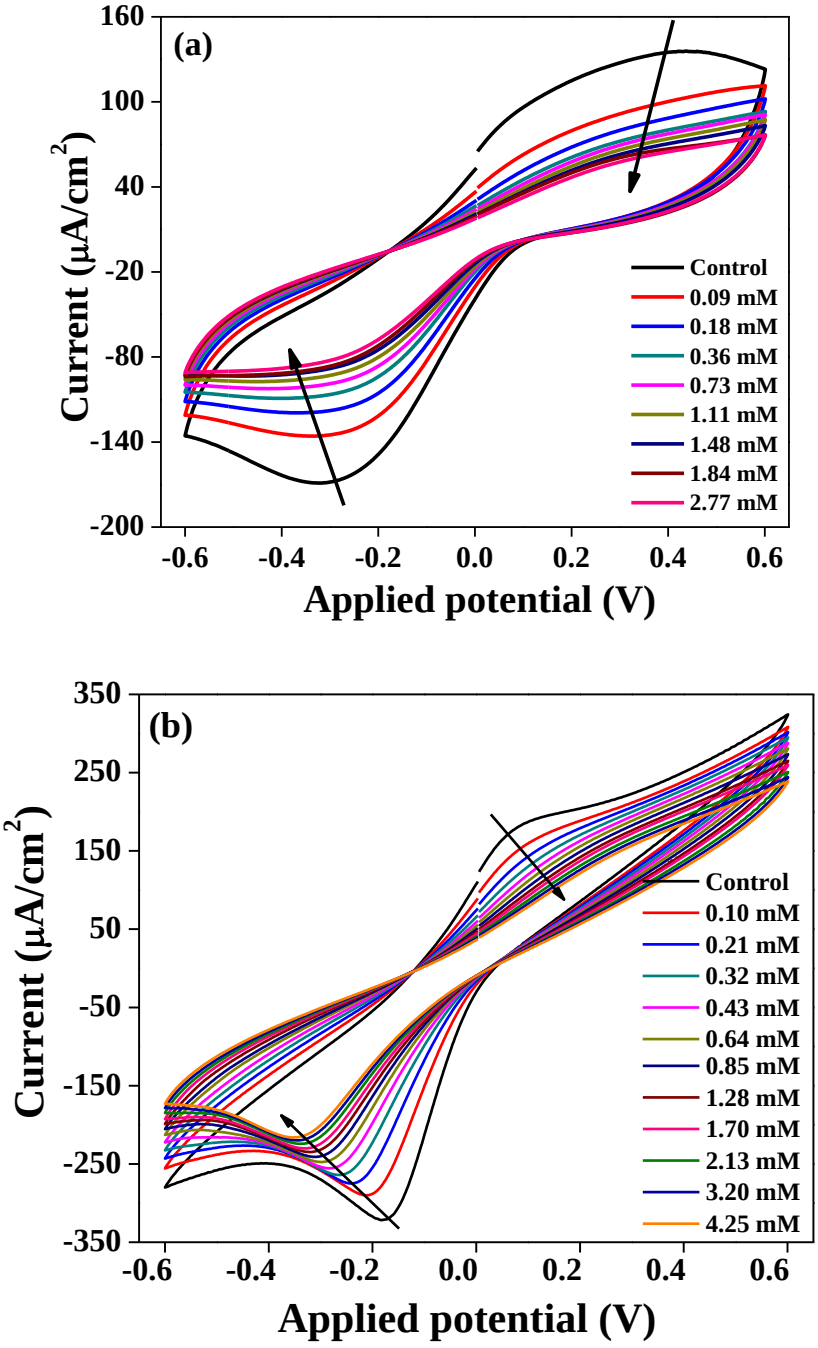

Fig. 8 Cyclic Voltammograms of in-situ (a) PANI and (b) PANI/G films in 0.1 M PBS solution at pH 7 at scan rate of 50 mVs^{-1} containing different concentrations of H_2O_2.

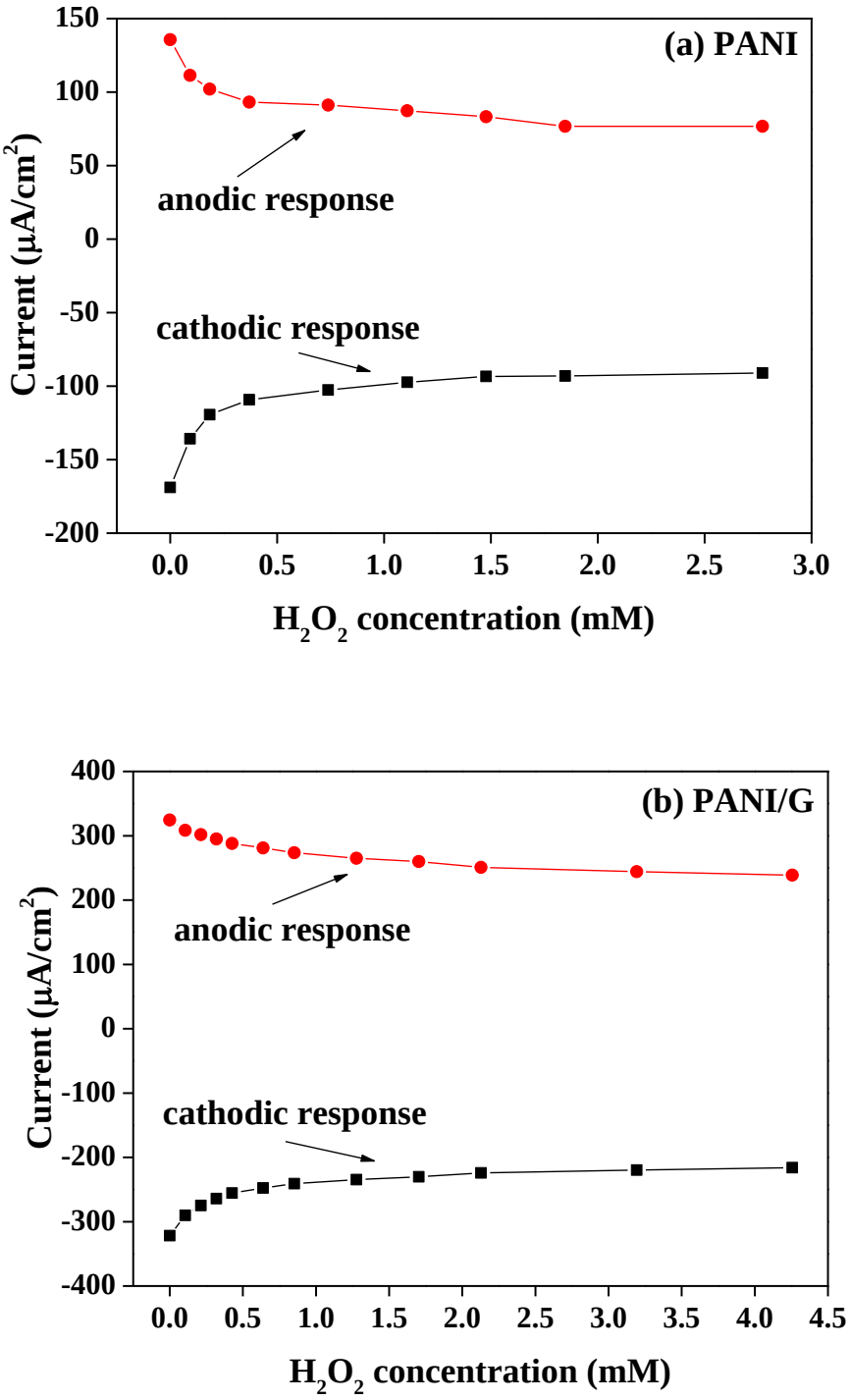

Fig. 9 Anodic and cathodic peak current responses for H_2O_2 determination using (a) PANI and (b) PANI/G films in 0.1 M PBS solution at pH 7 at scan rate of 50 mVs^{-1}.

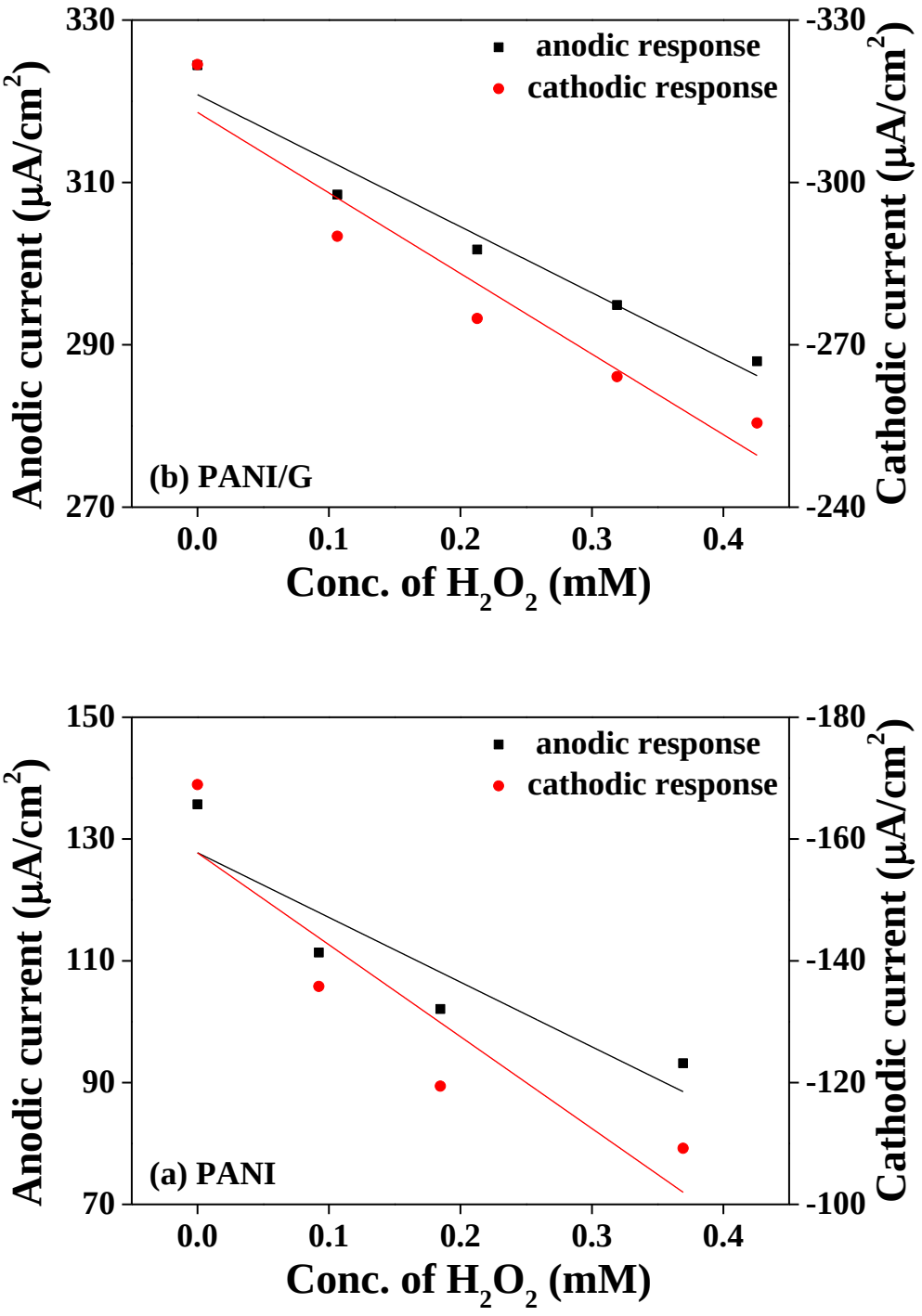

Fig. 10 Calibration curves for H_2O_2 detection using (a) PANI and (b) PANI/G thin films in 0.1 M PBS solution at pH 7 at scan rate of 50 mVs^{-1}.

Table 1. Characteristics of thin films prepared using in-situ method.

Order	Sample name	Thickness (nm)	Conductivity (S/cm)
1	PANI/ITO	141	5.38E+03
2	PANI/G_5 mg	30	6.65E+03
3	PANI/G_10 mg	126	6.84E+03
4	PAN/G_20 mg	26.7	6.97E+03

Table 2. Calculation method for LOD and LOQ values.

Order	Thin film		H_2O_2 conc. range (mM)	Equation of linear fit	SE	SD	LOD (mM)	LOQ (mM)
1	PANI/ITO	cathode	0 – 0.3694	$y = 150.9x - 157.7$ $R^2 = 0.829$	10.26	20.52	0.22	0.68
		anode		$y = -106.2x + 127.7$ $R^2 = 0.836$	7.03	14.06	0.22	0.66
2	PANI/G	cathode	0 – 0.4253	$y = 148.9x - 312.9$ $R^2 = 0.924$	6.42	14.36	0.14	0.43
		anode		$y = -81.3x + 320.8$ $R^2 = 0.958$	2.56	5.72	0.10	0.31

Table 3. Analytical performance of the PANI/G/ITO sensor for H_2O_2 determination in comparison to other reported electrochemical non-enzymatic sensors.

Order	Electrode	Technique	pH	Monitoring potential	LDR (µM)	Ref
1	$CuFe_2O_4$/RGO	Amperometry	5.0	-0.35 V*	2.00 – 200	[33]
2	Fc-TH/PIGE	Amperometry	7.0	-0.30 V**	0.57 - 785	[34]
3	GO-Cu^{2+}/GCE	Amperometry	7.4	-0.25 V*	5,000 – 85,000	[35]
4	CuS/GCE	Amperometry	7.4	-0.65 V*	10 – 1,900	[36]
5	MnO_2-GNSs/GCE	Amperometry	7.0	+0.70 V*	0.5 – 350	[37]
6	HMDE	SWV	3.2	-1.0 V*	0.0 – 120	[38]
7	PANI/G/ITO	CV	7.0	+0.09 V*	100.0 – 2,000	This study

$CuFe_2O_4$/RGO: graphene oxide and copper ferrite nanoparticles; Fc-TH/PIGE: paraffin wax impregnated graphite electrode modified with ferrocene/thionin; GO-Cu2+/GCE: graphene oxide/copper(2+) composite modified glassy carbon electrode; CuS/GCE: copper sulfide nanoparticle modified glassy carbon electrode; MnO2-GNSs/GCE: manganese dioxide-graphene nanosheets composite modified glassy carbon electrode; SWV: Square wave voltammetry; HMDE: hanging mercury drop electrode. *Ag|AgCl|KCl reference electrode. ** Saturated calomel electrode (SCE)